

---

**Research Articles: Behavioral/Cognitive**

**Stimulus-driven brain rhythms within the alpha band: The attentional-modulation conundrum**

Christian Keitel<sup>1</sup>, Anne Keitel<sup>1,2</sup>, Christopher SY Benwell<sup>1,2</sup>, Christoph Daube<sup>1</sup>, Gregor Thut<sup>1</sup> and Joachim Gross<sup>1,3</sup>

<sup>1</sup>*Institute of Neuroscience and Psychology, University of Glasgow, 62 Hillhead Street, Glasgow G12 8QB, UK*

<sup>2</sup>*Psychology, School of Social Sciences, University of Dundee, Scrymgeour Building, Dundee DD1 4HN, UK*

<sup>3</sup>*Institut für Biomagnetismus und Biosignalanalyse, Westfälische Wilhelms-Universität, Malmedyweg 15, 48149 Münster, Germany*

<https://doi.org/10.1523/JNEUROSCI.1633-18.2019>

Received: 29 June 2018

Revised: 16 January 2019

Accepted: 3 February 2019

Published: 19 February 2019

---

**Author contributions:** C.K., A.K., C.S.Y.B., C.D., G.T., and J.G. designed research; C.K. and A.K. performed research; C.K. and J.G. contributed unpublished reagents/analytic tools; C.K. and J.G. analyzed data; C.K. wrote the first draft of the paper; C.K., A.K., C.S.Y.B., C.D., G.T., and J.G. edited the paper; C.K., A.K., C.S.Y.B., C.D., G.T., and J.G. wrote the paper.

**Conflict of Interest:** The authors declare no competing financial interests.

Funded by a Wellcome Trust Joint Investigator Grant awarded to GT and JG (#098433/#098434). Lucy Dewhurst and Jennifer McAllister assisted in data collection. The experimental stimulation was realized using Cogent Graphics (RRID:SCR\_015672) developed by John Romaya at the Laboratory of Neurobiology, Wellcome Department of Imaging Neuroscience, University College London (UCL).

**Correspondence should be addressed to** corresponding author, [christian.keitel@glasgow.ac.uk](mailto:christian.keitel@glasgow.ac.uk)

**Cite as:** J. Neurosci 2019; 10.1523/JNEUROSCI.1633-18.2019

**Alerts:** Sign up at [www.jneurosci.org/alerts](http://www.jneurosci.org/alerts) to receive customized email alerts when the fully formatted version of this article is published.

Accepted manuscripts are peer-reviewed but have not been through the copyediting, formatting, or proofreading process.

Copyright © 2019 Keitel et al.

This is an open-access article distributed under the terms of the Creative Commons Attribution 4.0 International license, which permits unrestricted use, distribution and reproduction in any medium provided that the original work is properly attributed.

1 TITLE:

2 **Stimulus-driven brain rhythms within the alpha band: The attentional-modulation conundrum**

3

4 ABBREVIATED TITLE: Reversed attentional modulation of alpha and SSRs

5

AUTHORS:	Affiliation	ORCID	Twitter
Christian Keitel*	1	0000-0003-2597-5499	@KeiCetel
Anne Keitel	1,2	0000-0003-4498-0146	@anneke_sci
Christopher SY Benwell	1,2	0000-0002-4157-4049	@ChrisSYBenwell
Christoph Daube	1	0000-0002-1763-8508	@christophdaube
Gregor Thut	1	0000-0003-1313-4262	
Joachim Gross	1,3	0000-0002-3994-1006	@Joachim__Gross

6

7 AFFILIATIONS:

8 **1** – Institute of Neuroscience and Psychology, University of Glasgow, 62 Hillhead Street, Glasgow  
 9 G12 8QB, UK; **2** – Psychology, School of Social Sciences, University of Dundee, Scrymgeour Building,  
 10 Dundee DD1 4HN, UK; **3** – Institut für Biomagnetismus und Biosignalanalyse, Westfälische Wilhelms-  
 11 Universität, Malmedyweg 15, 48149 Münster, Germany

12 \* – corresponding author, christian.keitel@glasgow.ac.uk

13

14 KEYWORDS: alpha rhythm, entrainment, phase synchronisation, spatial attention, steady-state  
 15 response (SSR), frequency tagging

16

17 ACKNOWLEDGMENTS: Funded by a Wellcome Trust Joint Investigator Grant awarded to GT and JG  
 18 (#098433/#098434). Lucy Dewhurst and Jennifer McAllister assisted in data collection. The  
 19 experimental stimulation was realized using Cogent Graphics (RRID:SCR\_015672) developed by John  
 20 Romaya at the Laboratory of Neurobiology, Wellcome Department of Imaging Neuroscience,  
 21 University College London (UCL).

22

0 Table(s), 6 Figure(s), 0 Footnote(s)

23 **ABSTRACT**

24 Two largely independent research lines use rhythmic sensory stimulation to study visual processing.  
25 Despite the use of strikingly similar experimental paradigms, they differ crucially in their notion of  
26 the stimulus-driven periodic brain responses: One regards them mostly as synchronised (entrained)  
27 intrinsic brain rhythms; the other assumes they are predominantly evoked responses (classically  
28 termed steady-state responses, or SSRs) that add to the ongoing brain activity. This conceptual  
29 difference can produce contradictory predictions about, and interpretations of, experimental  
30 outcomes. The effect of spatial attention on brain rhythms in the alpha-band (8 – 13 Hz) is one such  
31 instance: alpha-range SSRs have typically been found to *increase* in power when participants focus  
32 their spatial attention on laterally presented stimuli, in line with a gain control of the visual evoked  
33 response. In nearly identical experiments, retinotopic *decreases* in entrained alpha-band power have  
34 been reported, in line with the inhibitory function of intrinsic alpha. Here we reconcile these  
35 contradictory findings by showing that they result from a small but far-reaching difference between  
36 two common approaches to EEG spectral decomposition. In a new analysis of previously published  
37 human EEG data, recorded during bilateral rhythmic visual stimulation, we find the typical SSR gain  
38 effect when emphasising stimulus-locked neural activity and the typical retinotopic alpha  
39 suppression when focusing on ongoing rhythms. These opposite but parallel effects suggest that  
40 spatial attention may bias the neural processing of dynamic visual stimulation via two  
41 complementary neural mechanisms.

42 **SIGNIFICANCE STATEMENT**

43 Attending to a visual stimulus strengthens its representation in visual cortex and leads to a  
44 retinotopic suppression of spontaneous alpha rhythms. To further investigate this process,  
45 researchers often attempt to phase-lock, or entrain, alpha through rhythmic visual stimulation under  
46 the assumption that this entrained alpha retains the characteristics of spontaneous alpha. Instead,  
47 we show that the part of the brain response that is phase-locked to the visual stimulation *increased*  
48 with attention (in line with steady-state evoked potentials), while the typical suppression was only  
49 present in non-stimulus-locked alpha activity. The opposite signs of these effects suggest that  
50 attentional modulation of dynamic visual stimulation relies on two parallel cortical mechanisms –  
51 retinotopic alpha suppression and increased temporal tracking.

52

53 **INTRODUCTION**

54 Cortical visual processing has long been studied using rhythmic sensory stimulation (Adrian and  
 55 Matthews, 1934; Walter et al., 1946; Regan, 1966). This type of stimulation drives continuous brain  
 56 responses termed steady-state responses (SSRs) that reflect the temporal periodicities in the  
 57 stimulation precisely. SSRs allow tracking of individual stimuli in multi-element displays (Vialatte et  
 58 al., 2010; Norcia et al., 2015). Further, they readily indicate cognitive biases of cortical visual  
 59 processing, such as the selective allocation of attention (Morgan et al., 1996; Keitel et al., 2013;  
 60 Stormer et al., 2014).

61 Although SSRs can be driven using a wide range of frequencies (Herrmann, 2001), stimulation at  
 62 alpha band frequencies (8 – 13 Hz) has stirred particular interest. Alpha rhythms dominate brain  
 63 activity in occipital visual cortices (Groppe et al., 2013; Keitel and Gross, 2016) and influence  
 64 perception (Benwell et al., 2017; Iemi et al., 2017; Samaha et al., 2017; Benwell et al., 2018).  
 65 Researchers have therefore used alpha-rhythmic visual stimulation in attempts to align the phase of  
 66 – or *entrain* – intrinsic alpha rhythms and consequently provided evidence for visual alpha  
 67 entrainment (Mathewson et al., 2012; Zauner et al., 2012; Spaak et al., 2014; Gulbinaite et al., 2017).  
 68 These findings suggest that at least part of the SSR driven by alpha-band stimulation should be  
 69 attributed to entrained alpha generators (Notbohm et al., 2016).

70 Some issues remain with such an account (Capilla et al., 2011; Keitel et al., 2014). For instance,  
 71 experiments have consistently reported SSR power increases when probing effects of spatial  
 72 selective attention on SSRs driven by lateralised hemifield stimuli (Müller et al., 1998a), also when  
 73 using alpha-band frequencies (Kim et al., 2007; Kashiwase et al., 2012; Keitel et al., 2013). However,  
 74 recent studies that used similar paradigms, but treated alpha-frequency SSRs as phase-entrained  
 75 alpha rhythms in line with an earlier study using rhythmic transcranial magnetic stimulation (Herring  
 76 et al., 2015), reported the opposite effect (Kizuk and Mathewson, 2017; Gulbinaite et al., 2019).  
 77 Oscillatory brain activity showed attentional modulations characteristic of the intrinsic alpha rhythm  
 78 during stimulation: Alpha power decreased over the hemisphere contralateral to the attended  
 79 position, an effect known to be part of a retinotopic alpha power lateralisation during selective  
 80 spatial attention (Worden et al., 2000; Kelly et al., 2006; Thut et al., 2006; Rihs et al., 2007; Capilla et  
 81 al., 2012). Briefly put, studies analysing SSRs show a power *increase*, whereas studies analysing  
 82 “entrained alpha” show a power *decrease* with attention.

83 Both neural responses originate from visual cortices contralateral to the hemifield position of the  
 84 driving stimuli (Keitel et al., 2013; Spaak et al., 2014). Assuming a single underlying neural process,  
 85 opposite attention effects therefore seemingly contradict each other. However, results in support of



alpha entrainment differed in how exactly responses to the periodic stimulation were quantified. Effects consistent with SSR modulation resulted from spectral decompositions performed on trial-averaged EEG waveforms. This approach tunes the resulting power estimate to the part of the neural response that is sufficiently time-locked to the stimulation (Tallon-Baudry et al., 1996; Delorme and Makeig, 2004). Effects consistent with alpha entrainment instead typically result from averages of single-trial spectral transforms, thus emphasising intrinsic non-phase-locked activity (Tallon-Baudry et al., 1998; Herrmann et al., 2004). Both approaches have been applied before to compare stimulus-evoked and induced brain rhythms in alpha (Moratti et al., 2007) and gamma frequency ranges (~40 Hz; Tallon-Baudry et al., 1998; Picton et al., 2003). Here we focussed on contrasting the attentional modulation of alpha during- and SSRs driven by an alpha-rhythmic stimulation.

We therefore compared the outcome of both approaches in a new analysis of previously reported EEG data (Keitel et al., 2017b). Participants viewed two lateralised stimuli, both flickering at alpha band frequencies (10 and 12 Hz). They were cued to focus on one of the two and perform a target detection task at the attended position. We quantified spectral power estimates according to both approaches described above from the same EEG data. Should the outcome depend on the approach taken, we expected to find the typical alpha power lateralisation (contralateral < ipsilateral) when averaging single-trial power spectra. In power spectra of trial-averaged EEG instead we expected the typical SSR power gain modulation in the opposite direction (contralateral > ipsilateral). Crucially, such an outcome would warrant a re-evaluation of stimulus-driven brain rhythms in the alpha range and intrinsic alpha as a unitary phenomenon (alpha entrainment).

[Insert Figure 1]

## METHODS

### Participants

For the present report, we re-analysed EEG data of 17 volunteers recorded in an earlier study (Keitel et al., 2017a). Participants (13 women; median age = 22 yrs, range = 19 – 32 yrs) declared normal or corrected-to-normal vision and no history of neurological diseases or injury. All procedures were approved by the ethics committee of the College of Science & Engineering at the University of Glasgow (application no. 300140020) and adhered to the guidelines for the treatment of human subjects in the Declaration of Helsinki. Volunteers received monetary compensation of £6/h. They gave informed written consent before participating in the experiment. Note that we excluded five additional datasets on grounds reported in the original study (four showed excessive eye movements, one underperformed in the task).

## 119 **Stimulation**

120 Participants viewed experimental stimuli on a computer screen (refresh rate = 100 frames per sec) at  
 121 a distance of 0.8 m that displayed a grey background (luminance =  $6.5 \text{ cd/m}^2$ ). Small concentric  
 122 circles in the centre of the screen served as a fixation point (*Figure 1*). Two blurry checkerboard  
 123 patches (horizontal/vertical diameter =  $4^\circ$  of visual angle) were positioned at an eccentricity of  $4.4^\circ$   
 124 from central fixation, one each in the lower left and lower right visual quadrants. Both patches  
 125 changed contrast rhythmically during trials: Stimulus contrast against the background was modulated  
 126 by varying patch peak luminance between  $7.5 \text{ cd/m}^2$  (minimum) and  $29.1 \text{ cd/m}^2$  (maximum).

127 On each screen refresh, peak luminance changed incrementally to approach temporally smooth  
 128 contrast modulations as opposed to a simple on-off flicker (Andersen and Muller, 2015). Further  
 129 details of the stimulation can be found in Keitel et al. (2017a). The contrast modulation followed a  
 130 10-Hz periodicity for the left and a 12-Hz periodicity for the right stimulus. Note that the experiment  
 131 featured further conditions displaying quasi-rhythmic contrast modulations in different frequency  
 132 bands. Corresponding results can be found in the original report and will not be considered in the  
 133 present analysis.

## 134 **Procedure and Task**

135 Participants performed the experiment in an acoustically dampened and electromagnetically  
 136 shielded chamber. In total, they were presented with 576 experimental trials, subdivided into 8  
 137 blocks with durations of  $\sim 5$  min each. Between blocks, participants took self-paced breaks. Prior to  
 138 the experiment, participants practiced the behavioural task (see below) for at least one block. After  
 139 each block they received feedback regarding their accuracy and response speed. The experiment was  
 140 comprised of 8 conditions (= 72 trials each) resulting from a manipulation of the two factors  
 141 attended position (left vs. right patch) and stimulation frequency (one rhythmic and three quasi-  
 142 rhythmic conditions) in a fully balanced design. Trials of different conditions were presented in  
 143 pseudo-random order. As stated above, the present study focussed on the two conditions featuring  
 144 fully rhythmic stimuli. Corresponding trials ( $N = 144$ ) were thus selected a posteriori from the full  
 145 design.

146 Single trials began with cueing participants to attend to the left or right stimulus for 0.5 sec, followed  
 147 by presentation of the dynamically contrast-modulating patches for 3.5 sec (*Figure 1*). After patch  
 148 offset, an idle period of 0.7 sec allowed participants to blink before the next trial started.

149 To control whether participants maintained a focus of spatial attention, they were instructed to  
 150 respond to occasional brief “flashes” (0.3 sec) of the cued stimulus (= targets) while ignoring similar

151 events in the other stimulus (= distracters). Targets and distracters occurred in one third of all trials  
 152 and up to 2 times in one trial with a minimum interval of 0.8 sec between subsequent onsets.  
 153 Detection was reported as speeded responses to flashes (recorded as space bar presses on a  
 154 standard keyboard).

#### 155 **Behavioural data recording and analyses**

156 Flash detections were considered a 'hit' when a response occurred from 0.2 to 1 sec after target  
 157 onset. Delays between target onsets and responses were considered reaction times (RT). Statistical  
 158 comparisons of mean accuracies (proportion of correct responses to the total number of targets and  
 159 distracters) and median RTs between experimental conditions were conducted and reported in  
 160 (2017a). In the present study, we did not consider the behavioural data further. Note that the  
 161 original statistical analysis found that task performance in Attend-Left and Attend-Right conditions  
 162 was comparable.

#### 163 **Electrophysiological data recording**

164 EEG was recorded from 128 scalp electrodes and digitally sampled at a rate of 512 Hz using a BioSemi  
 165 ActiveTwo system (BioSemi, Amsterdam, Netherlands). Scalp electrodes were mounted in an elastic  
 166 cap and positioned according to an extended 10-20-system (Oostenveld and Praamstra, 2001).  
 167 Lateral eye movements were monitored with a bipolar outer canthus montage (horizontal electro-  
 168 oculogram). Vertical eye movements and blinks were monitored with a bipolar montage of  
 169 electrodes positioned below and above the right eye (vertical electro-oculogram).

#### 170 **Electrophysiological data pre-processing**

171 From continuous data, we extracted epochs of 5 s, starting 1 s before patch onset using the MATLAB  
 172 (RRID:SCR\_001622) toolbox EEGLAB (Delorme and Makeig, 2004)( RRID:SCR\_016333). In further pre-  
 173 processing, we excluded epochs that corresponded to trials containing transient targets and  
 174 distracters (24 per condition) as well as epochs with horizontal and vertical eye movements  
 175 exceeding 20  $\mu$ V ( $\sim 2^\circ$  of visual angle) or containing blinks. For treating additional artefacts, such as  
 176 single noisy electrodes, we applied the 'fully automated statistical thresholding for EEG artefact  
 177 rejection' (FASTER; Nolan et al., 2010). This procedure corrected or discarded epochs with residual  
 178 artefacts based on statistical parameters of the data. Artefact correction employed a spherical-  
 179 spline-based channel interpolation. Epochs with more than 12 artefact-contaminated electrodes  
 180 were excluded from analysis.

181 From 48 available epochs per condition, we discarded a median of 14 epochs for the Attend-Left  
 182 conditions and 15 epochs for the Attend-Right conditions per participant with a between-subject

range of 6 to 28 (Attend-Left) and 8 to 31 epochs (Attend-Right). Within-subject variation of number of epochs per condition remained small with a median difference of 3 trials (maximum difference = 9 for one participant).

Subsequent analyses were carried out in Fieldtrip (Oostenveld et al., 2011)(RRID:SCR\_004849) in combination with custom-written routines. We extracted segments of 3 s starting 0.5 s after patch onset from pre-processed artefact-free epochs (5 s). Data prior to stimulation onset (1 s), only serving to identify eye movements shortly before and during cue presentation, were omitted. To attenuate the influence of stimulus-onset evoked activity on EEG spectral decomposition, the initial 0.5 s of stimulation were excluded. Lastly, because stimulation ceased after 3.5 s, we also discarded the final 0.5 s of original epochs.

### Electrophysiological data analyses – spectral decomposition

Artefact-free 3-sec epochs were converted to scalp current densities (SCDs), a reference-free measure of brain electrical activity (Ferree, 2006; Kayser and Tenke, 2015), by means of the spherical spline method (Perrin et al., 1987) as implemented in Fieldtrip (function *ft\_scalpcurrentdensity*, method 'spline',  $\lambda = 10^{-4}$ ). Detrended (i.e. mean and linear trend removed) SCD time series were then Tukey-tapered and subjected to Fourier transforms while employing zero-padding in order to achieve a frequency-resolution of 0.25 Hz. Crucially, from resulting complex Fourier spectra we calculated two sets of aggregate power spectra with slightly different approaches. First, we calculated power spectra as the average of squared absolute values of complex Fourier spectra ( $Z$ ) as follows:

$$onPOW(f) = \frac{1}{n} \sum_{i=1}^n |Z_i(f)|^2 \quad [1]$$

where *onPOW* is the classical power estimate for ongoing (intrinsic) oscillatory activity for frequency  $f$  and  $n$  is the number of trials. Secondly, we additionally calculated the squared absolute value of the averaged complex Fourier spectra according to:

$$evoPOW(f) = \left| \frac{1}{n} \sum_{i=1}^n Z_i(f) \right|^2 \quad [2]$$

The formula yields *evoPOW*, or evoked power, an estimate that is identical with the frequency-tagging standard approach of averaging per-trial EEG time series before spectral decomposition. This step is usually performed to retain only the truly phase-locked response to the stimulus (Tallon-Baudry et al., 1996). Note that both formulas only differ in the order in which weighted sums and absolute values are computed. Also note that formula [2] is highly similar to the calculation of inter-trial phase coherence (ITC), a popular measure of phase locking (Cohen, 2014; Gross, 2014; van

214 Diepen and Mazaheri, 2018). ITC calculation additionally includes a trial-by-trial amplitude  
 215 normalisation. To complement our analysis we thus quantified ITC according to:

$$216 \quad ITC(f) = \left| \frac{1}{n} \sum_{i=1}^n \frac{z_i(f)}{|z_i(f)|} \right| \quad [3]$$

217 For further analyses, power spectra were normalised by converting them to decibel scale, i.e. taking  
 218 the decadic logarithm, then multiplying by 10 (hereafter termed log power spectra). ITC was  
 219 converted to ITCz to reduce the bias introduced by differences in trial numbers between conditions  
 220 (Bonnefond and Jensen, 2012; Samaha et al., 2015).

### 221 **Alpha power – attentional modulation and lateralisation**

222 Spectra of ongoing power (*onPOW*), pooled over both experimental conditions and all electrodes,  
 223 showed a prominent peak in the alpha frequency range (*Figure 2*). We used mean log ongoing power  
 224 across the range of 8 – 13 Hz to assess intrinsic alpha power modulations by attention. Analysing  
 225 Attend-Right and Attend-Left conditions separately, yielded two alpha power topographies for each  
 226 participant. These were compared by means of cluster-based permutation statistics (Maris and  
 227 Oostenveld, 2007) using  $N = 5000$  random permutations. We clustered data across channel  
 228 neighbourhoods with an average size of 7.9 channels that were determined by triangulated sensor  
 229 proximity (function *ft\_prepare\_neighbours*, method ‘triangulation’). The resulting probabilities ( $P$ -  
 230 values) were corrected for two-sided testing. Subtracting left-lateralised (Attend-Left conditions)  
 231 from right-lateralised (Attend-Right) alpha power topographies, we found a right-hemispheric  
 232 positive and a left-hemispheric negative cluster of electrodes that was due to the retinotopic effects  
 233 of spatial attention on alpha power lateralisation (*Figure 3*), similar to an earlier re-analysis of the  
 234 other conditions of this experiment (Keitel et al., 2018).

235 Finally, we tested the difference between Attend-Left and Attend-Right conditions, i.e. attention  
 236 effects for left- and right-hemispheric clusters separately. To this end, we submitted alpha power  
 237 differences (contralateral hemifield attended minus ignored) to Bayesian one-sample t-tests against  
 238 zero (Rouder et al., 2009). Attention effects were further compared against each other by means of a  
 239 Bayesian paired-samples t-test as implemented in JASP (JASP-Team, 2018) (RRID:SCR\_015823) with a  
 240 Cauchy prior scaled to  $r = 0.5$ , putting more emphasis on smaller effects (Rouder et al., 2012;  
 241 Schonbrodt and Wagenmakers, 2017).

242 This procedure allowed us to quantify the evidence in favour of the null vs the alternative hypothesis  
 243 ( $H_0$  vs  $H_1$ ). For each test, the corresponding Bayes factor (called  $BF_{10}$ ) showed evidence for  $H_1$   
 244 (compared to  $H_0$ ) if it exceeded a value of 3, and no evidence for  $H_1$  if  $BF_{10} < 1$ , with the intervening  
 245 range 1 – 3 termed ‘anecdotal evidence’ by convention (Wagenmakers et al., 2011). Inversing  $BF_{10}$ , to

yield a quantity termed  $BF_{01}$ , served to quantify evidence in favour of  $H_0$  on the same scale. For  $BF_{10}$  and  $BF_{01}$ , values  $< 1$  were taken as inconclusive evidence for either hypothesis. Note that for the sake of brevity we report errors in BF estimates only when exceeding 0.001%.

[Insert Figure 2]

#### SSR power – attentional modulation

Spectra of evoked power, pooled over both experimental conditions and all electrodes, revealed periodic responses to the two stimuli at the respective stimulation frequencies, 10 and 12 Hz (Figure 2). Therefore, we assessed attention effects for these two spectral SSR representations. Two separate cluster-based permutation tests, one for each stimulation frequency, contrasted evoked power topographies between attended and ignored (= other stimulus attended) conditions. Two-sided tests were performed with the same parameters as for alpha power (see above).

Again, we found one electrode cluster carrying systematic attention effects per frequency. As for alpha, SSR power from these two clusters were subjected to separate Bayesian one-sample t-tests against zero (one-sided, attended  $>$  ignored) and compared against each other by means of a Bayesian paired-sample t-test (two-sided).

#### SSR inter-trial phase coherence – attentional modulation

We also evaluated a pure measure of neural phase-locking to the stimulation, SSR inter-trial phase coherence (ITC), because evoked power can be regarded as a hybrid measure depending on both the amplitude of the underlying rhythmic response and the consistency of its phase across trials. ITC indicates only the latter as SSRs are set to unit amplitude prior to summing across trials (see formula 3). ITC spectra, pooled over both experimental conditions and all electrodes, showed distinct neural phase-locking at the respective driving frequencies, 10 and 12 Hz (Figure 2). Cluster-based permutation testing confirmed topographic regions that showed systemic gain effects in ITC. Subsequently, the same Bayesian inference was applied to data from these clusters as for SSR power.

#### Correlation of alpha and SSR attention effects – group level

As a consequence of our counter-intuitive finding that SSR attention effects appeared strongest over occipital regions ipsi-lateral to the driving stimulus (see Results section *SSR power & inter-trial phase locking – attentional modulation* below), we explored a posteriori whether these effects could be explained by ipsilateral increases in alpha power during focussed attention. We correlated attention effects on alpha and SSR power using Bayesian inference (rank correlation coefficient Kendall's tau-b or  $\tau_b$ , beta-prior = 0.75) to test for a positive linear relationship. More specifically, we correlated the left-hemispheric alpha power suppression (Ignored minus Attended) with the 10-Hz SSR (evoked)

278 power attention effect (Attended minus Ignored) and the right-hemispheric alpha power suppression  
 279 with the 12-Hz SSR power attention effect. We opted for these combinations because the  
 280 corresponding effects overlapped topographically (see Results). Along with the correlation coefficient  
 281  $\rho$ , we report its 95%-Credible Interval (95%-CrI).

282 We also probed the linear relationship between alpha power and SSR ITC attention effects. Because  
 283 ITC gains were not clearly lateralised, we collapsed gain effects (Attended minus Ignored) across both  
 284 stimulation frequencies and correlated these with a hemisphere-collapsed alpha suppression index.  
 285 This index was quantified as the halved sum of left and right-hemispheric suppression effects as  
 286 retrieved from significant clusters in the topographical analysis of alpha power differences (Attend  
 287 Left minus Attend Right), shown in *Figure 3*. Again, we expected a positive correlation here if alpha  
 288 power suppression influenced phase-locking to visual stimulation. For means of comparison, we  
 289 repeated this analysis with attention effects on SSR power collapsed across frequencies.

290 [Insert Figure 3]

#### 291 **Alpha and SSR attention effects – subject level regression**

292 The relationship between alpha power (lateralisation) and SSR attentional modulation was further  
 293 subjected to a more fine-grained analysis considering within-subject variability across single trials  
 294 and allowing for a better control of between-subject differences in alpha and SSR power. We  
 295 assumed that if the SSR attention effect (i.e. the ipsilateral SSR power gain) was a mere consequence  
 296 of the co-localised alpha power increase then these two effects should co-vary across trials. For this  
 297 analysis we recalculated single-trial alpha power and SSR evoked power / ITC estimates at each EEG  
 298 sensor and for both conditions in each subject based on the same artefact-removed EEG epochs and  
 299 using the same spectral decomposition as described above. Because ITC is not defined for single  
 300 trials, we used a Jackknife approach that computed single trial estimates in a leave-one-out  
 301 procedure and allowed for subsequent evaluation of inter-trial variability (Richter et al., 2015). For  
 302 consistency, we computed similar alpha-power Jackknife estimates. From these estimates, we  
 303 calculated attention effects as all possible pairwise differences between trials of different conditions  
 304 (Attend Left vs Attend Right), yielding distributions of alpha power hemispheric lateralisation and SSR  
 305 evoked power / ITC attentional modulation (for 10 & 12 Hz SSRs separately). To validate this  
 306 approach, we used it to reproduce alpha power and SSR attention effects described below (data not  
 307 shown, reproducible via code in online repository (Keitel et al., 2017b)).

308 We then tested for a linear relationship between both z-scored measures by subjecting them to a  
 309 robust linear regression (MATLAB function 'robustfit', default options), carried out for each EEG  
 310 sensor separately. The obtained subject-specific regression coefficients  $\theta$  (slopes) were entered into



a group statistical test. We tested slopes against zero (i.e. no linear relationship) by means of cluster-based permutation tests (two-tailed), clustering across EEG sensors. Four tests were carried out in total; one for each regression of alpha power lateralisation with SSR evoked power or SSR ITC attentional modulation, and separately for 10 & 12 Hz SSR, respectively. This procedure was supplemented by sensor-by-sensor Bayesian t-tests (Rouder et al., 2009) to quantify the evidence in favour of a linear vs no relationship (see Methods section *Alpha power – attentional modulation and lateralisation* regarding Bayesian inference).

## RESULTS

### Ongoing alpha power – attentional modulation and lateralisation

The power of the ongoing alpha rhythm lateralised with the allocation of spatial attention to left and right stimuli. A topographic map of the differences in alpha power between Attend-Left and Attend-Right conditions shows significant left- and right-hemispheric electrode clusters (*Figure 3*). These clusters signify retinotopic alpha power modulation when participants attended to left vs right stimulus positions (right cluster:  $t_{\text{sum}} = -21.454$ ,  $P = 0.026$ ; left cluster:  $t_{\text{sum}} = 81.264$ ,  $P = 0.002$ ). The differences are further illustrated in power spectra pooled over electrodes of each cluster (*Figure 3*). As predicted, alpha power at each cluster was lower when participants attended to the contralateral stimulus. Bayesian inference confirmed the alpha power attention effect for the right ( $M = 0.806$  dB,  $SEM = 0.216$ ;  $BF_{10} = 21.17$ ) and left cluster ( $M = 0.790$  dB,  $SEM = 0.133$ ;  $BF_{10} = 906.36$ ). Both effects were of comparable magnitude ( $BF_{01} = 4.009 \pm 0.007$ ).

### SSR power & inter-trial phase locking – attentional modulation

Crucially, we found the opposite pattern when looking at SSRs, i.e. the exact same data but with a slightly different focus on oscillatory brain activity that was time-locked to the stimulation (compare formulas 1 and 2): SSRs showed increased power when the respective driving stimulus was attended versus ignored (*Figure 4*). The power of neural responses evoked by our stimuli (SSRs) was at least one order of magnitude smaller than ongoing alpha power on average (difference > 10dB, i.e. between 10 – 100 times). Nevertheless, SSRs could be clearly identified as distinct peaks in (evoked) power and ITC spectra. Consistent with the retinotopic projection to early visual cortices, topographical distributions of both measures showed a focal maxima contra-lateral to the respective stimulus positions that were attended (*Figure 2*). Counter-intuitively though, maximum attention effects on SSR power did not coincide topographically with sites that showed maximum SSR power overall (compare scalp maps in *Figure 2 & 4*). Also, due to their rather ipsilateral scalp distributions

(with respect to the attended location), SSR attention effects did not match topographies of attention-related decreases in ongoing alpha power (compare scalp maps in *Figures 3 & 4*). The 10-Hz SSR driven by the left-hemifield stimulus showed a left-hemispheric power increase when attended ( $t_{\text{sum}} = 15.837$ ,  $P = 0.059$ ). Similarly, attention increased the power of the 12-Hz SSR driven by the right-hemifield stimulus in a right-hemispheric cluster ( $t_{\text{sum}} = 53.282$ ,  $P < 0.001$ ). Bayesian inference confirmed the attention effect on 10-Hz ( $M = 3.727$  dB,  $SEM = 0.919$ ;  $BF_{10} = 37.05$ ) and 12-Hz SSR power ( $M = 4.473$  dB,  $SEM = 0.841$ ;  $BF_{10} = 329.75$ ) averaged within clusters. Both effects were of comparable magnitude ( $BF_{01} = 3.443 \pm 0.005$ ).

SSR phase-locking (quantified as ITCz) also increased with attention to the respective stimulus. In contrast to evoked power, topographical representations of these effects showed greater overlap with the sites that showed maximum phase-locking in general (*Figure 4*). For both frequencies, ITCz increased in central occipital clusters (10 Hz:  $t_{\text{sum}} = 41.351$ ,  $P = 0.004$ ; 12 Hz:  $t_{\text{sum}} = 31.116$ ,  $P = 0.012$ ). Again, Bayesian inference confirmed the attention effect on 10-Hz ( $M = 1.386$  au,  $SEM = 0.297$ ;  $BF_{10} = 105.71$ , one-sided) and 12-Hz ITCz ( $M = 1.824$  au,  $SEM = 0.451$ ;  $BF_{10} = 36.11$ , one-sided). Evidence for a greater attention effect on 12-Hz than on 10-Hz ITC remained inconclusive ( $BF_{10} = 0.473$ ).

[Insert Figure 4]

#### Correlation of alpha and SSR attention effects – group level

Lastly, we tested whether the SSR attention gain effects were mere reflections of the topographically coinciding ipsilateral ongoing alpha power increase during focussed attention that co-occurred with the contralateral ongoing alpha-power decrease (*Figure 3*). Speaking against this account, Bayesian inference provided moderate evidence against the expected positive correlations between the left-hemispheric alpha attention effect and the 10-Hz SSR attention effect ( $\tau_b = -0.221$ , 95%-CrI = [0.002 0.269];  $BF_{01} = 5.811$ ) and between the right-hemispheric alpha attention effect and the 12-Hz SSR attention effect ( $\tau_b = -0.088$ , 95%-CrI = [0.004 0.315];  $BF_{01} = 3.904$ ). These relationships are further illustrated by corresponding linear fits in *Figure 5*.

Following this analysis, we further explored the relationship between spatially non-overlapping decreases in alpha-power contralateral to the attended position and the ipsilateral SSR power gain effects. For the lack of a specific hypothesis about the sign of the correlation in this case, we quantified the evidence for any relationship (two-sided test). The results remained inconclusive for a correlation between the left-hemispheric alpha attention effect and the right-hemispheric 12-Hz SSR attention effect ( $\tau_b = 0.235$ , 95%-CrI = [-0.110 0.487];  $BF_{01} = 1.280$ ) and between the right-

hemispheric alpha attention effect and the left-hemispheric 10-Hz SSR attention effect ( $\tau_b = 0.103$ , 95%-CrI = [-0.218 0.383];  $BF_{01} = 2.400$ ).

[Insert Figure 5]

Finally, we repeated this analysis for attention effects on inter-trial phase coherence (ITC). Because SSR ITC attention effects did not show a clear topographical lateralisation (*Figure 4*), they were collapsed across driving frequencies (10 & 12 Hz). Again, findings were inconclusive when looking into the correlation between these aggregate SSR ITC gain effects and a hemisphere-collapsed alpha suppression index ( $\tau_b = -0.059$ , 95%-CrI = [-0.349 0.251];  $BF_{01} = 2.653$ ). Correlating collapsed attention effects of SSR evoked power with the same pooled alpha suppression index yielded identical results regarding the rank correlation (also see linear fits in *Figure 5*).

#### Alpha and SSR attention effects – subject level regression

A more fine-grained analysis of single-trial co-variation of alpha power lateralisation and SSR gain effects during focussed spatial attention largely corroborated the group level results. Clustering across EEG sensors, we found that only the 12-Hz SSR evoked power attention effect and alpha lateralisation co-varied systematically across participants at occipital sites (permutation test,  $T_{sum} = -17.517$ ,  $p = 0.023$ ). The negative sign of the slope however contradicted the expected positive relationship (*Figure 6a*). Neither 10-Hz SSR evoked power nor SSR ITC (both frequencies) revealed similar systematic relationships with alpha power.

Additionally, we used Bayesian inference on the distributions of individual regression slopes (indicating the linear relationship between alpha and SSR attention effects) by sensor to quantify the plausibility of either  $H_1$  or  $H_0$  in scalp maps (*Figure 6b*). We further overlaid these scalp maps with electrode clusters showing SSR attention effects (compare with *Figure 4*). Average Bayes factors (Bfs) within clusters indicated that evidence for or against any type of linear relationship remained inconclusive for 10-Hz (mean  $Bf_{01} = 1.422$  range = 0.639 – 2.343) and 12-Hz SSR evoked power (mean  $Bf_{01} = 1.245$  range = 0.153 – 3.673), although it should be mentioned that the 12-Hz cluster contained a local maximum ( $Bf_{10} = 1/Bf_{01} = 6.534$ ) that coincided topographically with the effect identified by the cluster-based permutation test. For ITC evidence favoured  $H_0$ , i.e. the absence of any relationship with 10-Hz (mean  $Bf_{01} = 3.040$ , range = 1.861 – 4.014) and 12-Hz SSR ( $Bf_{01} = 3.030$ , range = 1.391 – 4.016) was 3 times more likely given our data.

Our findings show a fine distinction between SSR evoked power and ITC gain effects with respect to a possible connection to alpha lateralisation in that only the latter provided conclusive evidence against such a relationship. As a likely explanation, SSR evoked power still contains residual alpha

activity that confounds tests for covariation. Conversely, the single-trial power normalisation step undertaken during the calculation of SSR ITC makes it less susceptible to this confound. Taken together, the findings of this analysis do not support a positive linear relationship of alpha lateralisation and SSR gain effects (especially on ITC). Therefore, it is unlikely that the counter-intuitive topography of SSR attentional modulation is a reflection of alpha power lateralisation during focused spatial attention.

[Insert Figure 6]

## DISCUSSION

We found that two common spectral measures of alpha-band EEG during alpha-rhythmic visual stimulation reflect effects of spatial attention with opposite signs. In the following we discuss how this finding supports the notion of two complementary neural mechanisms governing the cortical processing of dynamic visual input.

### Analysis approach determines sign of attentional modulation

When focussing on the spectral representation of ongoing EEG power, we observed the prototypical broad peak in the alpha frequency range (8 – 13 Hz; *Figure 2*). Moreover, alpha power decreased over the hemisphere contralateral to the attended stimulus position, indicating a functional disinhibition of cortical areas representing task-relevant regions of the visual field (Worden et al., 2000; Kelly et al., 2006; Thut et al., 2006). Concurrently, alpha power increased over the ipsilateral hemisphere, actively suppressing irrelevant and possibly distracting input (Rihs et al., 2007; Capilla et al., 2012).

A second approach focussed on the SSRs, i.e. strictly stimulus-locked rhythmic EEG components. As in classical frequency-tagging studies, we found spectrally distinct SSRs at the stimulation frequencies (here 10 and 12 Hz). These two concurrent rhythmic brain responses thus precisely reflected the temporal dynamics of the visual stimulation. Notably, SSR evoked power was between one to two orders of magnitude (10 – 100 times) lower than ongoing-alpha power. Smaller evoked power also explained why SSRs remained invisible in spectra of ongoing activity. They were likely masked by the broad alpha peak (*Figure 2*; Covic et al., 2017). Note that this is a result of the relatively low-intensity stimulation used here. Stimulation of higher intensity can evoke SSRs that are readily visible in power spectra of ongoing activity (Gulbinaite et al., 2019).

Crucially, we examined SSRs for effects of focused spatial attention. Visual cortical regions contralateral to the respective driving stimuli showed maximum SSR evoked power. We would

439 expect to observe a decrease in SSR evoked power with attention (Kizuk and Mathewson, 2017;  
 440 Gulbinaite et al., 2019) under the assumption that SSRs are frequency-specific neural signatures of a  
 441 local entrainment of intrinsic alpha generators (Spaak et al., 2014; Notbohm et al., 2016) and exhibit  
 442 similar functional characteristics. Instead, we found that SSR evoked power increased in line with  
 443 earlier reports (Kim et al., 2007; Kashiwase et al., 2012; Keitel et al., 2013).

444 Note however that these attentional gain effects did not coincide topographically with scalp  
 445 locations of maximum SSR evoked power (*Figure 4*). Instead, they were most pronounced over  
 446 hemispheres ipsilateral to the position of the respective driving stimuli and thus co-localised with  
 447 ipsilateral alpha power increases (*Figure 3*). Two control analyses showed that these effects were  
 448 unlikely to be related (*Figure 5 & 6*). We have described the apparent counter-intuitive lateralisation  
 449 of this effect before (Keitel et al., 2017a) when comparing scalp distributions by means of Attended-  
 450 minus-Unattended contrasts (Keitel et al., 2017a). In that case, expecting attention effects to emerge  
 451 at sites of maximum SSR power entails the implicit assumption that attention only acts as a local  
 452 response gain mechanism. Alternatively, neural representations of attended stimuli could access  
 453 higher order visual processing (Lithari et al., 2016) and a gain in spatial extent could then produce  
 454 seemingly ipsilateral effects when evaluating topographical differences as observed here. However,  
 455 previous cortical source reconstructions of SSRs in lateralised stimulus situations have unequivocally  
 456 localised maximum effects of visuo-spatial attention to contralateral visual cortices (Müller et al.,  
 457 1998b; Lauritzen et al., 2010; Keitel et al., 2013). Considering the limited spatial resolution of EEG,  
 458 and that SSR inter-trial phase coherence showed yet another non-lateralised topographical  
 459 distribution for gain effects (*Figure 4*), warrants a dedicated neuroimaging analysis of the underlying  
 460 cortical sources that generate these attentional modulations.

#### 461 **Opposite but co-occurring attention effects suggest interplay of distinct attention-related** 462 **processes**

463 Our analysis compared attention effects between “ongoing” spectral power within the alpha  
 464 frequency band and a quantity termed SSR “evoked power” that is commonly used in frequency  
 465 tagging research (Colon et al., 2012; Porcu et al., 2013; Stormer et al., 2014; Walter et al., 2016;  
 466 Martinovic and Andersen, 2018). This term is somewhat misleading because it conflates a power  
 467 estimate with the consistency of the phase of the SSR across trials of the experiment. Inter-trial  
 468 phase consistency (ITC) has been used to quantify SSRs before (Ruhnau et al., 2016). It is closely  
 469 related to evoked power but involves an extra normalisation term that abolishes (or at least greatly  
 470 attenuates) the power contribution (Cohen, 2014; Gross, 2014). Note that in a noisy, finite signal  
 471 such as the typical second(s)-long EEG epoch, there will be a positive relationship between the power

472 and inter-trial phase consistency at any frequency as is shown by the greater than zero noise floor in  
 473 our ITC spectra (Figure 4). Also note that ITC only measures SSRs meaningfully if the  
 474 neurophysiological signal contains a periodic component at the stimulation frequency.

475 The effects of attention on SSR evoked power and ITC are typically interchangeable (Covic et al.,  
 476 2017; Keitel et al., 2017a). In fact, increased ITC, or phase synchronisation, has been considered the  
 477 primary effect of attention on stimulus-driven periodic brain responses (Kim et al., 2007; Kranczioch,  
 478 2017). Looking at spectral power and ITC separately, as two distinct aspects of rhythmic brain  
 479 activity, therefore resolves the attentional modulation conundrum: Seemingly opposing attention-  
 480 related effects likely index different but parallel influences on cortical processing of rhythmic visual  
 481 input. To avoid confusion, we therefore suggest opting for ITC (or related measures, e.g. the cosine  
 482 similarity index (Chou and Hsu, 2018)) instead of “evoked power” to evaluate SSRs.

483 Incorporating our findings into an account that regards SSRs primarily as stimulus-driven entrainment  
 484 of intrinsic alpha rhythms would require demonstrating how a decrease in alpha-band power (i.e. the  
 485 contralateral alpha suppression) can co-occur with increased SSR phase synchronisation.  
 486 Alternatively, stimulus-locked (“evoked”) and intrinsic alpha rhythms could be considered distinct  
 487 processes (Freunberger et al., 2009; Sauseng, 2012). Consequentially, alpha range SSRs could  
 488 predominantly reflect an early cortical mechanism for the tracking of fluctuations in stimulus-specific  
 489 visual input per se (Keitel et al., 2017a) without the need to assume entrainment (Capilla et al., 2011;  
 490 Keitel et al., 2014).

491 The underlying neural mechanism might similarly work for a range of rhythmic and quasi-rhythmic  
 492 stimuli owing to the fact that visual cortex comprises a manifold of different feature detectors that  
 493 closely mirror changes along the dimensions of colour, luminance, contrast, spatial frequency and  
 494 more (Buracas et al., 1998; Blaser et al., 2000; Martinovic and Andersen, 2018). Most importantly, for  
 495 (quasi-)rhythmic sensory input, attention to the driving stimulus may increase neural phase-locking  
 496 to the stimulus to allow for enhanced tracking of its dynamics, i.e. increased fidelity. This effect has  
 497 been observed for quasi-rhythmic low-frequency visual speech signals (Crosse et al., 2015; Park et al.,  
 498 2016; Hauswald et al., 2018) and task-irrelevant visual stimuli at attended vs ignored spatial locations  
 499 (Keitel et al., 2017a).

500 Concurrent retinotopic biasing of visual processing through alpha suppression and stronger neural  
 501 phase-locking to attended stimuli could therefore be regarded as complimentary mechanisms. Both  
 502 could act to facilitate the processing of behaviourally relevant visual input in parallel. In this context,  
 503 SSRs would constitute a special case and easy-to-quantify periodic signature of early visual cortices  
 504 tracking stimulus dynamics over time. Intrinsic alpha suppression instead may gate the access of

505 sensory information to superordinate visual processing stages (Jensen and Mazaheri, 2010; Zumer et  
 506 al., 2014) and enhanced ipsilateral alpha power may additionally attenuate irrelevant and possibly  
 507 distracting stimuli at ignored locations (Capilla et al., 2012).

508 A neuronal implementation may work like this: During rest or inattention, occipital neuronal  
 509 populations synchronise with a strong internal, thalamo-cortical pacemaker (alpha). During attentive  
 510 processing of sensory input, retinotopic alpha suppression releases specific neuronal sub-populations  
 511 from an internal reign and allows them to track the stimulus dynamics at attended locations. A  
 512 related mechanism has been observed in the striatum, where local field potentials are dominated by  
 513 synchronous oscillatory activity across large areas (Courtemanche et al., 2003). However, during task  
 514 performance focal neuronal populations were found to disengage from this global synchronicity in a  
 515 consistent and task-specific manner. At the level of EEG/MEG recordings, such a mechanism could  
 516 lead to task-related decrease of oscillatory power but increase of coherence or ITC, as observed in  
 517 the current study and previously in the sensorimotor system (Gross et al., 2005; Schoffelen et al.,  
 518 2005; Schoffelen et al., 2011).

519 Whereas such an account challenges the occurrence of strictly stimulus-driven alpha entrainment, it  
 520 may still allow alpha to exert temporally precise top-down influences during predictable and  
 521 behaviourally relevant rhythmic stimulation – a process that itself could be subject to entrainment  
 522 (Thut et al., 2011; Nobre et al., 2012; Haegens and Zion Golumbic, 2018; Zoefel et al., 2018).

## 523 **Conclusion**

524 Our findings reconcile seemingly contradictory findings regarding spatial attention effects on alpha-  
 525 rhythmic activity, assumed to be entrained by periodic visual stimulation, and SSRs. Focusing on  
 526 spectral power or phase consistency of the EEG during visual stimulation yielded reversed attention  
 527 effects in the same dataset. Our findings encourage a careful and consistent choice of measures of  
 528 ongoing brain dynamics (here power) or measures of stimulus-related activity (here ITC), that should  
 529 be critically informed by the experimental question, when studying the effects of visuo-spatial  
 530 selective attention on the cortical processing of dynamic (quasi-) rhythmic visual stimulation. Again,  
 531 we emphasise that both common data analysis approaches taken here can be equally valid and  
 532 legitimate, yet they likely represent distinct neural phenomena. These can occur simultaneously, as  
 533 in our case, and may index distinct cortical processes that work in concert to facilitate the processing  
 534 of visual stimulation at attended locations.



535

536 **Competing interests**

537 The authors declare no competing interests.

538

539 **Author contributions**

540 CK designed research, performed research, analysed data and wrote the article. JG designed research

541 analysed data and wrote the article. AK, CSYB, CD and GT designed research and wrote the article.

542

543 **Data accessibility**

544 EEG data, pre-processed in Fieldtrip format, that underlie all analyses reported here and a

545 corresponding MATLAB analysis script are available on the Open Science Framework, [osf.io/apsyf](https://osf.io/apsyf)

546 (Keitel et al., 2017b).

547

548 **References**

549

550 Adrian ED, Matthews BH (1934) The interpretation of potential waves in the cortex. *J Physiol* 81:440-  
551 471.552 Andersen SK, Muller MM (2015) Driving steady-state visual evoked potentials at arbitrary frequencies  
553 using temporal interpolation of stimulus presentation. *BMC Neurosci* 16:95.554 Benwell CSY, Keitel C, Harvey M, Gross J, Thut G (2018) Trial-by-trial co-variation of pre-stimulus EEG  
555 alpha power and visuospatial bias reflects a mixture of stochastic and deterministic effects.  
556 *Eur J Neurosci* 48:2566-2584.557 Benwell CSY, Tagliabue CF, Veniero D, Cecere R, Savazzi S, Thut G (2017) Prestimulus EEG Power  
558 Predicts Conscious Awareness But Not Objective Visual Performance. *eNeuro* 4.559 Blaser E, Pylyshyn ZW, Holcombe AO (2000) Tracking an object through feature space. *Nature*  
560 408:196-199.561 Bonnefond M, Jensen O (2012) Alpha oscillations serve to protect working memory maintenance  
562 against anticipated distracters. *Curr Biol* 22:1969-1974.563 Buracas GT, Zador AM, DeWeese MR, Albright TD (1998) Efficient discrimination of temporal patterns  
564 by motion-sensitive neurons in primate visual cortex. *Neuron* 20:959-969.565 Capilla A, Pazo-Alvarez P, Darriba A, Campo P, Gross J (2011) Steady-state visual evoked potentials  
566 can be explained by temporal superposition of transient event-related responses. *PLoS One*  
567 6:e14543.

- 568 Capilla A, Schoffelen J-M, Paterson G, Thut G, Gross J (2012) Dissociated  $\alpha$ -Band Modulations in the  
 569 Dorsal and Ventral Visual Pathways in Visuospatial Attention and Perception. *Cerebral*  
 570 *Cortex*.
- 571 Chou EP, Hsu SM (2018) Cosine similarity as a sample size-free measure to quantify phase clustering  
 572 within a single neurophysiological signal. *J Neurosci Methods* 295:111-120.
- 573 Cohen MX (2014) Analyzing neural time series data: theory and practice. Cambridge, Massachusetts:  
 574 MIT Press.
- 575 Colon E, Nozaradan S, Legrain V, Mouraux A (2012) Steady-state evoked potentials to tag specific  
 576 components of nociceptive cortical processing. *Neuroimage* 60:571-581.
- 577 Courtemanche R, Fujii N, Graybiel AM (2003) Synchronous, focally modulated beta-band oscillations  
 578 characterize local field potential activity in the striatum of awake behaving monkeys.  
 579 *Journal of Neuroscience* 23:11741-11752.
- 580 Covic A, Keitel C, Porcu E, Schroger E, Muller MM (2017) Audio-visual synchrony and spatial attention  
 581 enhance processing of dynamic visual stimulation independently and in parallel: A  
 582 frequency-tagging study. *Neuroimage* 161:32-42.
- 583 Crosse MJ, Butler JS, Lalor EC (2015) Congruent Visual Speech Enhances Cortical Entrainment to  
 584 Continuous Auditory Speech in Noise-Free Conditions. *J Neurosci* 35:14195-14204.
- 585 Delorme A, Makeig S (2004) EEGLAB: an open source toolbox for analysis of single-trial EEG dynamics  
 586 including independent component analysis. *J Neurosci Methods* 134:9-21.
- 587 Ferree TC (2006) Spherical splines and average referencing in scalp electroencephalography. *Brain*  
 588 *Topogr* 19:43-52.
- 589 Freunberger R, Fellinger R, Sauseng P, Gruber W, Klimesch W (2009) Dissociation between phase-  
 590 locked and nonphase-locked alpha oscillations in a working memory task. *Hum Brain Mapp*  
 591 30:3417-3425.
- 592 Groppe DM, Bickel S, Keller CJ, Jain SK, Hwang ST, Harden C, Mehta AD (2013) Dominant frequencies  
 593 of resting human brain activity as measured by the electrocorticogram. *Neuroimage*  
 594 79:223-233.
- 595 Gross J (2014) Analytical methods and experimental approaches for electrophysiological studies of  
 596 brain oscillations. *J Neurosci Methods* 228:57-66.
- 597 Gross J, Pollok B, Dirks M, Timmermann L, Butz M, Schnitzler A (2005) Task-dependent oscillations  
 598 during unimanual and bimanual movements in the human primary motor cortex and SMA  
 599 studied with magnetoencephalography. *Neuroimage* 26:91-98.
- 600 Gulbinaite R, Roostendaal D, VanRullen R (2019) Attention differentially modulates the amplitude of  
 601 resonance frequencies in the visual cortex. *bioRxiv*.

- 602 Gulbinaite R, van Viegen T, Wieling M, Cohen MX, VanRullen R (2017) Individual Alpha Peak  
 603 Frequency Predicts 10 Hz Flicker Effects on Selective Attention. *J Neurosci* 37:10173-10184.
- 604 Haegens S, Zion Golumbic E (2018) Rhythmic facilitation of sensory processing: A critical review.  
 605 *Neurosci Biobehav Rev* 86:150-165.
- 606 Hauswald A, Lithari C, Collignon O, Leonardelli E, Weisz N (2018) A Visual Cortical Network for  
 607 Deriving Phonological Information from Intelligible Lip Movements. *Curr Biol* 28:1453-1459  
 608 e1453.
- 609 Herring JD, Thut G, Jensen O, Bergmann TO (2015) Attention Modulates TMS-Locked Alpha  
 610 Oscillations in the Visual Cortex. *J Neurosci* 35:14435-14447.
- 611 Herrmann CS (2001) Human EEG responses to 1-100 Hz flicker: resonance phenomena in visual  
 612 cortex and their potential correlation to cognitive phenomena. *Exp Brain Res* 137:346-353.
- 613 Herrmann CS, Munk MH, Engel AK (2004) Cognitive functions of gamma-band activity: memory  
 614 match and utilization. *Trends Cogn Sci* 8:347-355.
- 615 Iemi L, Chaumon M, Crouzet SM, Busch NA (2017) Spontaneous Neural Oscillations Bias Perception  
 616 by Modulating Baseline Excitability. *J Neurosci* 37:807-819.
- 617 JASP-Team (2018) JASP. In, 0.8.2 Edition.
- 618 Jensen O, Mazaheri A (2010) Shaping functional architecture by oscillatory alpha activity: gating by  
 619 inhibition. *Front Hum Neurosci* 4:186.
- 620 Kashiwase Y, Matsumiya K, Kuriki I, Shioiri S (2012) Time courses of attentional modulation in neural  
 621 amplification and synchronization measured with steady-state visual-evoked potentials. *J*  
 622 *Cogn Neurosci* 24:1779-1793.
- 623 Kayser J, Tenke CE (2015) On the benefits of using surface Laplacian (current source density)  
 624 methodology in electrophysiology. *Int J Psychophysiol* 97:171-173.
- 625 Keitel A, Gross J (2016) Individual Human Brain Areas Can Be Identified from Their Characteristic  
 626 Spectral Activation Fingerprints. *PLoS Biology* 14:e1002498.
- 627 Keitel C, Quigley C, Ruhnau P (2014) Stimulus-Driven Brain Oscillations in the Alpha Range:  
 628 Entrainment of Intrinsic Rhythms or Frequency-Following Response? *Journal of*  
 629 *Neuroscience* 34:10137-10140.
- 630 Keitel C, Thut G, Gross J (2017a) Visual cortex responses reflect temporal structure of continuous  
 631 quasi-rhythmic sensory stimulation. *Neuroimage* 146:58-70.
- 632 Keitel C, Andersen SK, Quigley C, Muller MM (2013) Independent Effects of Attentional Gain Control  
 633 and Competitive Interactions on Visual Stimulus Processing. *Cerebral Cortex* 23:940-946.
- 634 Keitel C, Benwell CSY, Thut G, Gross J (2017b) Alpha during quasi-periodic visual stimulation. In. *Open*  
 635 *Science Framework*.

- 636 Keitel C, Benwell CSY, Thut G, Gross J (2018) No changes in parieto-occipital alpha during neural  
637 phase locking to visual quasi-periodic theta-, alpha-, and beta-band stimulation. *Eur J*  
638 *Neurosci*.
- 639 Kelly SP, Lalor EC, Reilly RB, Foxe JJ (2006) Increases in alpha oscillatory power reflect an active  
640 retinotopic mechanism for distracter suppression during sustained visuospatial attention. *J*  
641 *Neurophysiol* 95:3844-3851.
- 642 Kim YJ, Grabowecy M, Paller KA, Muthu K, Suzuki S (2007) Attention induces synchronization-based  
643 response gain in steady-state visual evoked potentials. *Nat Neurosci* 10:117-125.
- 644 Kizuk SA, Mathewson KE (2017) Power and Phase of Alpha Oscillations Reveal an Interaction between  
645 Spatial and Temporal Visual Attention. *J Cogn Neurosci* 29:480-494.
- 646 Krancioch C (2017) Individual differences in dual-target RSVP task performance relate to  
647 entrainment but not to individual alpha frequency. *PLoS One* 12:e0178934.
- 648 Lauritzen TZ, Ales JM, Wade AR (2010) The effects of visuospatial attention measured across visual  
649 cortex using source-imaged, steady-state EEG. *J Vis* 10.
- 650 Lithari C, Sanchez-Garcia C, Ruhnau P, Weisz N (2016) Large-scale network-level processes during  
651 entrainment. *Brain Res* 1635:143-152.
- 652 Maris E, Oostenveld R (2007) Nonparametric statistical testing of EEG- and MEG-data. *J Neurosci*  
653 *Methods* 164:177-190.
- 654 Martinovic J, Andersen SK (2018) Cortical summation and attentional modulation of combined  
655 chromatic and luminance signals. *Neuroimage* 176:390-403.
- 656 Mathewson KE, Prudhomme C, Fabiani M, Beck DM, Lleras A, Gratton G (2012) Making waves in the  
657 stream of consciousness: entraining oscillations in EEG alpha and fluctuations in visual  
658 awareness with rhythmic visual stimulation. *J Cogn Neurosci* 24:2321-2333.
- 659 Moratti S, Clementz BA, Gao Y, Ortiz T, Keil A (2007) Neural mechanisms of evoked oscillations:  
660 stability and interaction with transient events. *Hum Brain Mapp* 28:1318-1333.
- 661 Morgan ST, Hansen JC, Hillyard SA (1996) Selective attention to stimulus location modulates the  
662 steady-state visual evoked potential. *Proceedings of the National Academy of Sciences of*  
663 *the United States of America* 93:4770-4774.
- 664 Müller MM, Teder-Sälejärvi W, Hillyard SA (1998a) The time course of cortical facilitation during cued  
665 shifts of spatial attention. *Nat Neurosci* 1:631-634.
- 666 Müller MM, Picton TW, Valdes-Sosa P, Riera J, Teder-Salejarvi WA, Hillyard SA (1998b) Effects of  
667 spatial selective attention on the steady-state visual evoked potential in the 20-28 Hz range.  
668 *Brain Res Cogn Brain Res* 6:249-261.

- 669 Nobre AC, Rohenkohl G, Stokes M (2012) Nervous anticipation: top-down biasing across space and  
670 time. In: *Cognitive Neuroscience of Attention*, 2 Edition (Posner MI, ed), pp 159-186. New  
671 York: Guilford.
- 672 Nolan H, Whelan R, Reilly RB (2010) FASTER: Fully Automated Statistical Thresholding for EEG artifact  
673 Rejection. *J Neurosci Methods* 192:152-162.
- 674 Norcia AM, Appelbaum LG, Ales JM, Cottareau BR, Rossion B (2015) The steady-state visual evoked  
675 potential in vision research: A review. *J Vis* 15:4.
- 676 Notbohm A, Kurths J, Herrmann CS (2016) Modification of Brain Oscillations via Rhythmic Light  
677 Stimulation Provides Evidence for Entrainment but Not for Superposition of Event-Related  
678 Responses. *Front Hum Neurosci* 10:10.
- 679 Oostenveld R, Praamstra P (2001) The five percent electrode system for high-resolution EEG and ERP  
680 measurements. *Clin Neurophysiol* 112:713-719.
- 681 Oostenveld R, Fries P, Maris E, Schoffelen JM (2011) FieldTrip: Open source software for advanced  
682 analysis of MEG, EEG, and invasive electrophysiological data. *Comput Intell Neurosci*  
683 2011:156869.
- 684 Park H, Kayser C, Thut G, Gross J (2016) Lip movements entrain the observers' low-frequency brain  
685 oscillations to facilitate speech intelligibility. *Elife* 5.
- 686 Perrin F, Pernier J, Bertrand O, Giard MH, Echallier JF (1987) Mapping of scalp potentials by surface  
687 spline interpolation. *Electroencephalogr Clin Neurophysiol* 66:75-81.
- 688 Picton TW, John MS, Purcell DW, Plourde G (2003) Human auditory steady-state responses: the  
689 effects of recording technique and state of arousal. *Anesth Analg* 97:1396-1402.
- 690 Porcu E, Keitel C, Muller MM (2013) Concurrent visual and tactile steady-state evoked potentials  
691 index allocation of inter-modal attention: a frequency-tagging study. *Neurosci Lett* 556:113-  
692 117.
- 693 Regan D (1966) Some characteristics of average steady-state and transient responses evoked by  
694 modulated light. *Electroencephalogr Clin Neurophysiol* 20:238-248.
- 695 Richter CG, Thompson WH, Bosman CA, Fries P (2015) A jackknife approach to quantifying single-trial  
696 correlation between covariance-based metrics undefined on a single-trial basis.  
697 *Neuroimage* 114:57-70.
- 698 Rihs TA, Michel CM, Thut G (2007) Mechanisms of selective inhibition in visual spatial attention are  
699 indexed by alpha-band EEG synchronization. *Eur J Neurosci* 25:603-610.
- 700 Rouder JN, Morey RD, Speckman PL, Province JM (2012) Default Bayes factors for ANOVA designs.  
701 *Journal of Mathematical Psychology* 56:356-374.

- 702 Rouder JN, Speckman PL, Sun DC, Morey RD, Iverson G (2009) Bayesian t tests for accepting and  
 703 rejecting the null hypothesis. *Psychonomic Bulletin & Review* 16:225-237.
- 704 Ruhnau P, Keitel C, Lithari C, Weisz N, Neuling T (2016) Flicker-Driven Responses in Visual Cortex  
 705 Change during Matched-Frequency Transcranial Alternating Current Stimulation. *Front Hum*  
 706 *Neurosci* 10:184.
- 707 Samaha J, Iemi L, Postle BR (2017) Prestimulus alpha-band power biases visual discrimination  
 708 confidence, but not accuracy. *Conscious Cogn* 54:47-55.
- 709 Samaha J, Bauer P, Cimaroli S, Postle BR (2015) Top-down control of the phase of alpha-band  
 710 oscillations as a mechanism for temporal prediction. *Proc Natl Acad Sci U S A* 112:8439-  
 711 8444.
- 712 Sauseng P (2012) Brain oscillations: phase-locked EEG alpha controls perception. *Curr Biol* 22:R306-  
 713 308.
- 714 Schoffelen JM, Oostenveld R, Fries P (2005) Neuronal coherence as a mechanism of effective  
 715 corticospinal interaction. *Science* 308:111-113.
- 716 Schoffelen JM, Poort J, Oostenveld R, Fries P (2011) Selective movement preparation is subserved by  
 717 selective increases in corticomuscular gamma-band coherence. *J Neurosci* 31:6750-6758.
- 718 Schonbrodt FD, Wagenmakers EJ (2017) Bayes factor design analysis: Planning for compelling  
 719 evidence. *Psychon Bull Rev*.
- 720 Spaak E, de Lange FP, Jensen O (2014) Local entrainment of alpha oscillations by visual stimuli causes  
 721 cyclic modulation of perception. *J Neurosci* 34:3536-3544.
- 722 Stormer VS, Alvarez GA, Cavanagh P (2014) Within-hemifield competition in early visual areas limits  
 723 the ability to track multiple objects with attention. *J Neurosci* 34:11526-11533.
- 724 Tallon-Baudry C, Bertrand O, Delpuech C, Pernier J (1996) Stimulus specificity of phase-locked and  
 725 non-phase-locked 40 Hz visual responses in human. *J Neurosci* 16:4240-4249.
- 726 Tallon-Baudry C, Bertrand O, Peronnet F, Pernier J (1998) Induced gamma-band activity during the  
 727 delay of a visual short-term memory task in humans. *J Neurosci* 18:4244-4254.
- 728 Thut G, Schyns PG, Gross J (2011) Entrainment of perceptually relevant brain oscillations by non-  
 729 invasive rhythmic stimulation of the human brain. *Front Psychol* 2:170.
- 730 Thut G, Nietzel A, Brandt SA, Pascual-Leone A (2006) Alpha-band electroencephalographic activity  
 731 over occipital cortex indexes visuospatial attention bias and predicts visual target detection.  
 732 *J Neurosci* 26:9494-9502.
- 733 van Diepen RM, Mazaheri A (2018) The Caveats of observing Inter-Trial Phase-Coherence in Cognitive  
 734 Neuroscience. *Sci Rep* 8:2990.

- 735 Vialatte FB, Maurice M, Dauwels J, Cichocki A (2010) Steady-state visually evoked potentials: focus on  
 736 essential paradigms and future perspectives. *Prog Neurobiol* 90:418-438.
- 737 Wagenmakers EJ, Wetzels R, Borsboom D, van der Maas HL (2011) Why psychologists must change  
 738 the way they analyze their data: the case of psi: comment on Bem (2011). *J Pers Soc Psychol*  
 739 100:426-432.
- 740 Walter S, Keitel C, Muller MM (2016) Sustained Splits of Attention within versus across Visual  
 741 Hemifields Produce Distinct Spatial Gain Profiles. *J Cogn Neurosci* 28:111-124.
- 742 Walter WG, Dovey VJ, Shipton H (1946) Analysis of the Electrical Response of the Human Cortex to  
 743 Photoc Stimulation. *Nature* 158:540-541.
- 744 Worden MS, Foxe JJ, Wang N, Simpson GV (2000) Anticipatory biasing of visuospatial attention  
 745 indexed by retinotopically specific alpha-band electroencephalography increases over  
 746 occipital cortex. *J Neurosci* 20:RC63.
- 747 Zauner A, Fellinger R, Gross J, Hanslmayr S, Shapiro K, Gruber W, Muller S, Klimesch W (2012) Alpha  
 748 entrainment is responsible for the attentional blink phenomenon. *Neuroimage* 63:674-686.
- 749 Zoefel B, Ten Oever S, Sack AT (2018) The Involvement of Endogenous Neural Oscillations in the  
 750 Processing of Rhythmic Input: More Than a Regular Repetition of Evoked Neural Responses.  
 751 *Front Neurosci* 12:95.
- 752 Zumer JM, Scheeringa R, Schoffelen JM, Norris DG, Jensen O (2014) Occipital alpha activity during  
 753 stimulus processing gates the information flow to object-selective cortex. *PLoS Biology*  
 754 12:e1001965.
- 755
- 756



757 **Figure captions**

758 **Figure 1** Stimulus schematics and trial time course. (a) shows the time course of one trial with a cue  
 759 displayed for 0.5 sec (here: Attend Right), followed by the bilateral visual stimulation for 3.5 sec. Left  
 760 (L) stimulus contrast fluctuated with a rate of 10 Hz and Right (R) stimulus contrast at 12 Hz. Targets  
 761 that participants were instructed to respond to were slightly altered versions of the stimuli (see  
 762 inset) that were displayed occasionally for 0.3 sec. (b) Rhythmic visual stimulation was achieved by a  
 763 frame-by-frame adjustment of global stimulus contrast (through local luminance changes) as  
 764 exemplified here in one representative cycle.

765 **Figure 2** EEG spectral decomposition. (a) Power spectra collapsed across conditions and all electrode  
 766 positions below the sagittal midline for single subjects (light grey lines) and group averages (strong  
 767 black line). Note the characteristic alpha peaks in the frequency range of 8 – 13 Hz. Inset scalp map  
 768 shows topographical distribution of alpha power on a dB scale based on scalp current densities. (b)  
 769 Same as in (a) but for ‘evoked’ power. Distinct peaks are visible at stimulation frequencies 10 & 12 Hz  
 770 (dashed vertical orange lines across plots). Inset scalp maps show topographical distributions of SSR  
 771 power at 10 & 12 on a dB scale. Note the difference in scale between ongoing power in (a) and  
 772 evoked power (b). (c) Same as in (a) but for inter-trial phase-locking (ITCz). Inset scalp maps show  
 773 topographical distributions of SSR ITCz at 10 & 12.

774 **Figure 3** Allocation of spatial attention produces retinotopic alpha power modulation. The scalp map  
 775 (top, center) depicts alpha power lateralisation (Attend Left – Attend right conditions) on a dB scale.  
 776 Black dots indicate left- and right-hemispheric electrode-clusters that showed a consistent difference  
 777 in group statistics (two-tailed cluster-based permutation tests). Left and right spectra illustrate alpha  
 778 power differences in respective clusters when the contralateral hemifield was attended (Att) versus  
 779 ignored (Ign). The bottom grey inset depicts the distribution of individual alpha power suppression  
 780 effects (Ignored minus Attended) within left (L) and right (R) hemisphere clusters in the 8 – 13 Hz  
 781 band. Boxplots indicate interquartile ranges (boxes) and medians (coloured vertical intersectors).  
 782 Dots below show individual effects (1 dot = 1 participant).

783 **Figure 4** Attention effects on SSR evoked power (evoPow) and SSR inter-trial phase coherence. (a)  
 784 SSR evoked power spectra show systematic power differences at the presentation frequency (10 Hz)  
 785 of the left stimulus when it was attended (dark red) versus ignored (orange). The inset scalp map  
 786 illustrates the topographical distribution of the attention effects. Power spectra were averaged  
 787 across electrodes (black dots in scalp maps) that showed consistent attention effects in group  
 788 statistics (two-tailed cluster-based permutation tests) for Attended and Ignored conditions  
 789 separately. (b) Same as in (a) but for the 12-Hz stimulus presented in the right visual hemifield. (c,d)  
 790 Same as in (a,b) but using ITCz as a measure of SSR inter-trial phase coherence.

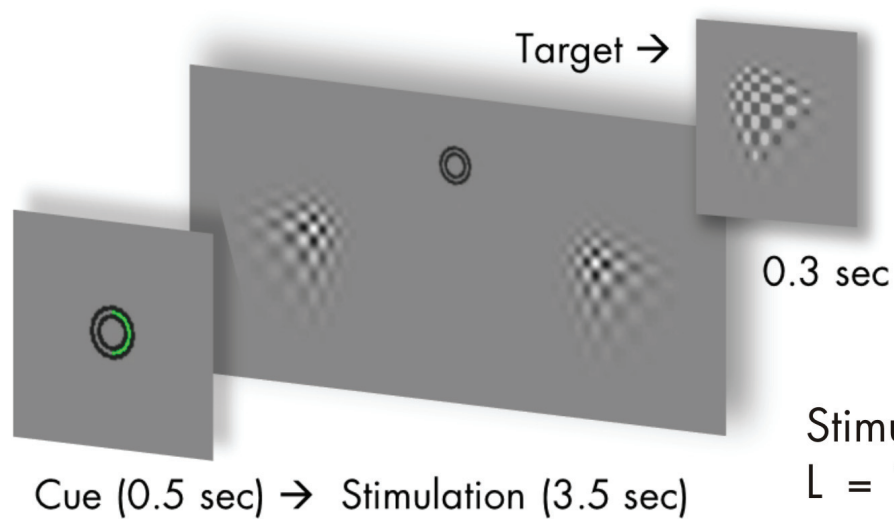
791 **Figure 5** Relationships between attention effects on alpha power and SSRs. (a) Individual 10-Hz (left  
 792 stimulus) SSR evoked power gain (Attended minus Ignored; z-scored, y-axis) as a function of alpha  
 793 suppression (Ignored minus Attended; z-scored, x axis) in overlapping left-hemispheric parieto-  
 794 occipital electrode clusters. Grey dots represent participants. Coloured lines depict a straight line fit  
 795 and its confidence interval (dashed lines). Goodness of fit of the linear model provided as  $R^2$  along  
 796 with corresponding P-Value. As confirmed by additional tests, both attention effects do not show a  
 797 positive linear relationship that would be expected if the ipsilateral SSR power gain effect was a  
 798 consequence of the ipsilateral alpha suppression. (b) Same as in (a), but for the 12 Hz SSR driven by  
 799 the right stimulus in overlapping right-hemispheric parieto-occipital electrode clusters. (c,d) Similar  
 800 to (a) but for attention-related gain effects on SSR ITCz (z-scored, y-axis) in (c) and gain effects on SSR  
 801 evoked power in (d), both collapsed across electrode clusters showing 10- and 12-Hz SSR attention  
 802 effects. Alpha suppression was collapsed across left- and right-hemispheric electrode clusters (see  
 803 Figure 3).

804 **Figure 6** Summary of subject-level analysis of the linear relationship between alpha power and SSR  
 805 attentional modulation. **(a)** depicts the topographical distribution of group-averaged (N=17)  
 806 regression coefficients  $\beta$  (slopes) for SSR evoked power (top row) and SSR inter-trial coherence (ITC,  
 807 bottom row), separated by SSR frequencies 10 Hz (left column) and 12 Hz (right column). Hot colours  
 808 indicate a positive linear relationship and cool colours a negative relationship. Black dots in the upper  
 809 right panel indicate a cluster of electrodes showing a systematic effect ( $p < 0.05$ , cluster-based  
 810 permutation test) absent in tests illustrated in the other 3 panels. **(b)** Results of sensor-by-sensor  
 811 group-level Bayesian inference (Bayesian t-tests) of regression slopes against zero, plotted as  
 812 topographies on a  $\log(BF_{10})$  scale. Plots arranged as in (a). Red colours indicate stronger evidence for  
 813  $H_1$ , grey colours indicate stronger evidence for  $H_0$ . Black lines in the colour scale below scalp maps  
 814 denote thresholds that signal moderate evidence for  $H_0$  ( $\log(1/3) = -1.099$ ) or  $H_1$  ( $\log(3) = 1.099$ ) by  
 815 convention. Superimposed black dots indicate clusters showing systematic attention effects on SSR  
 816 evoked power / ITC as depicted in *Figure 4* for comparison.

817

**a**

Stimulation



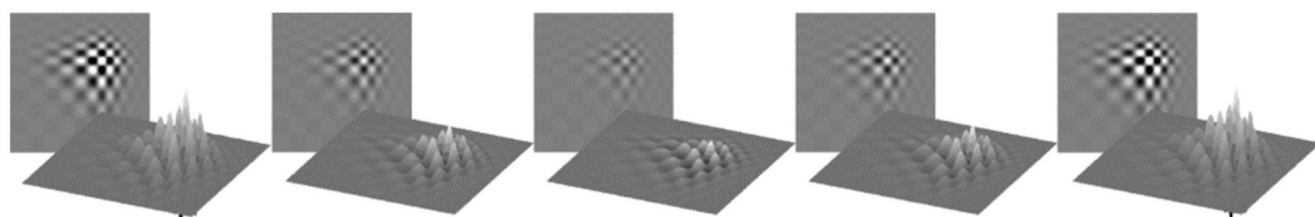
Stimulus frequency:

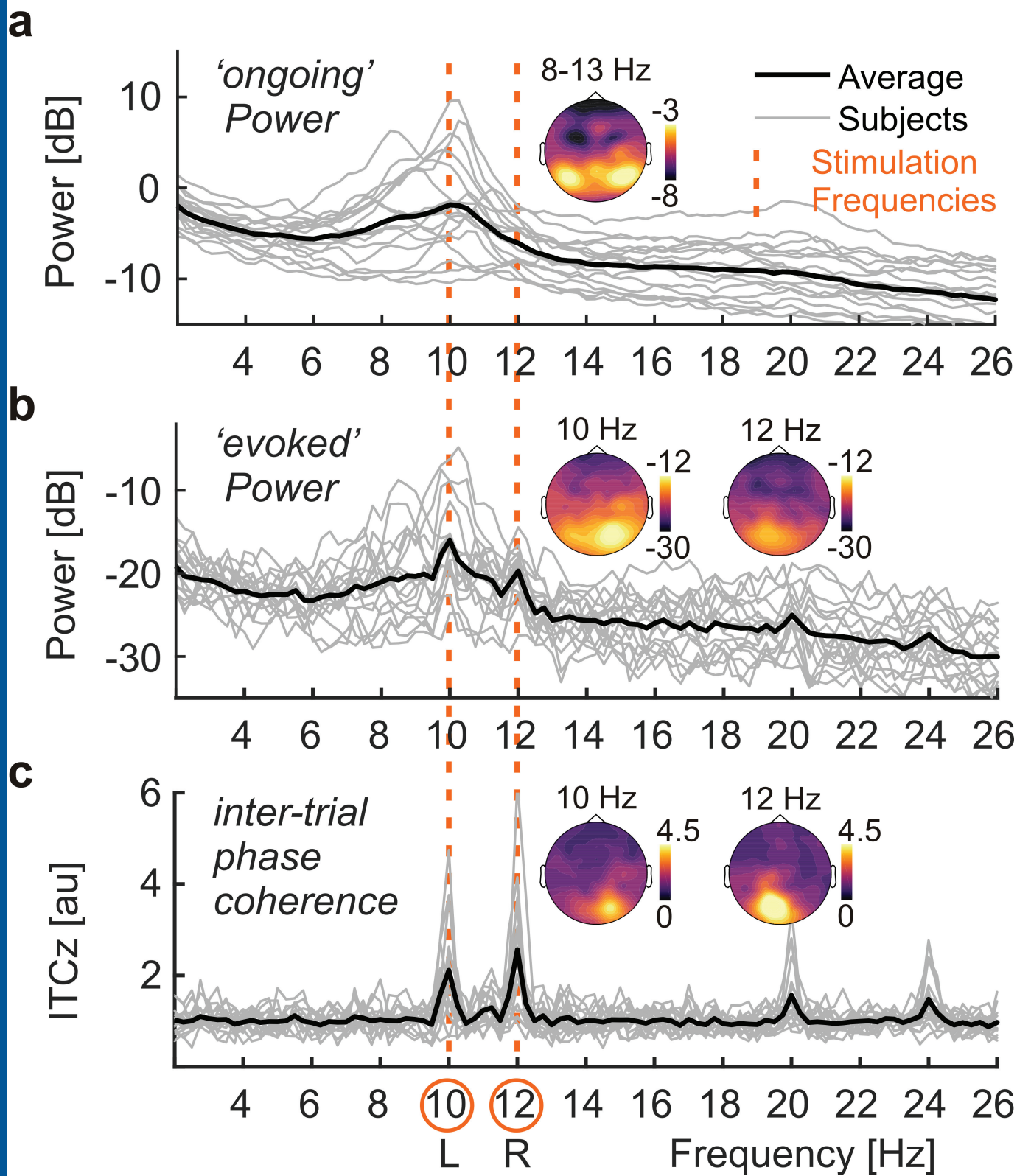
L = 10 Hz

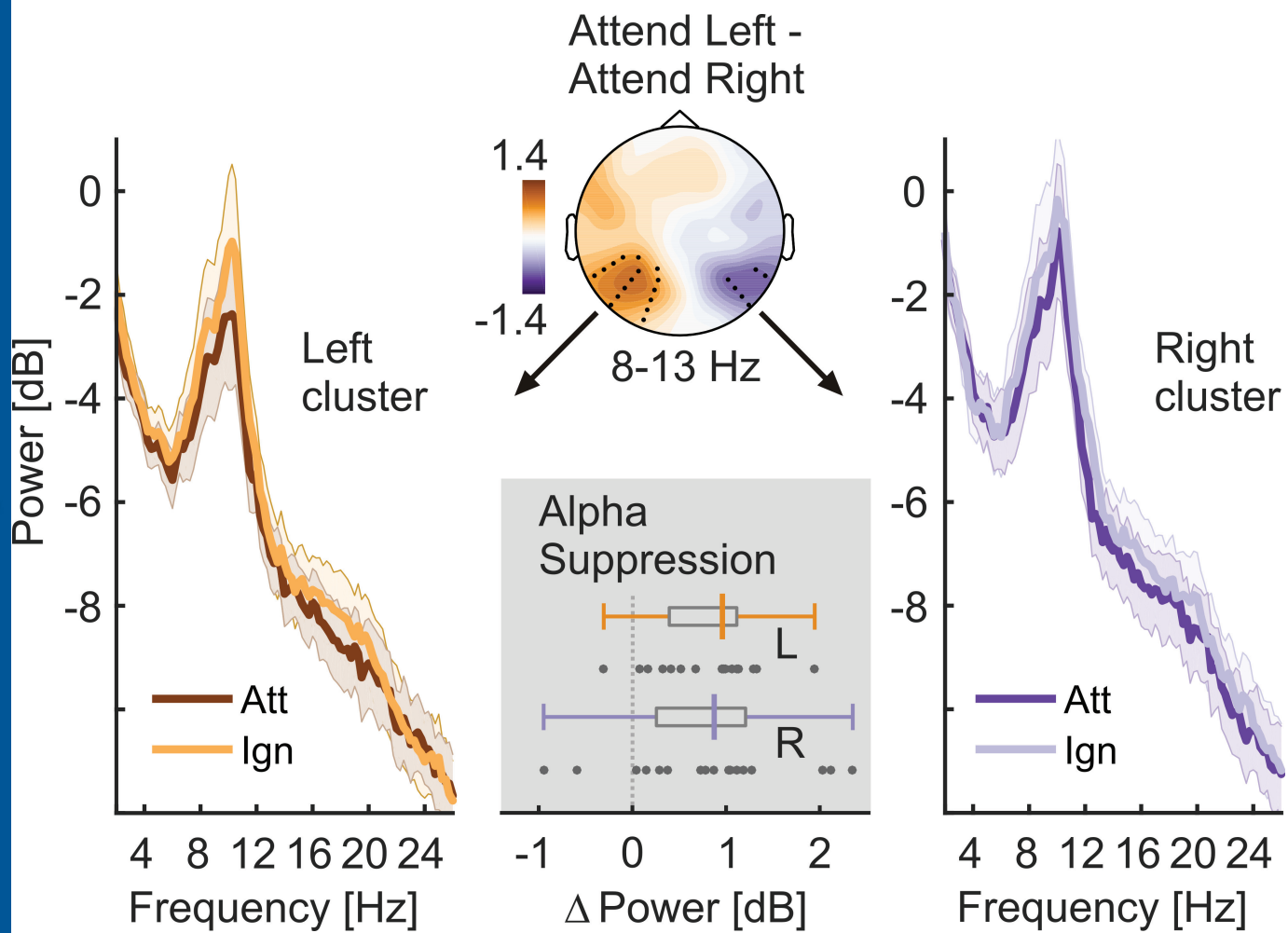
R = 12 Hz

**b**

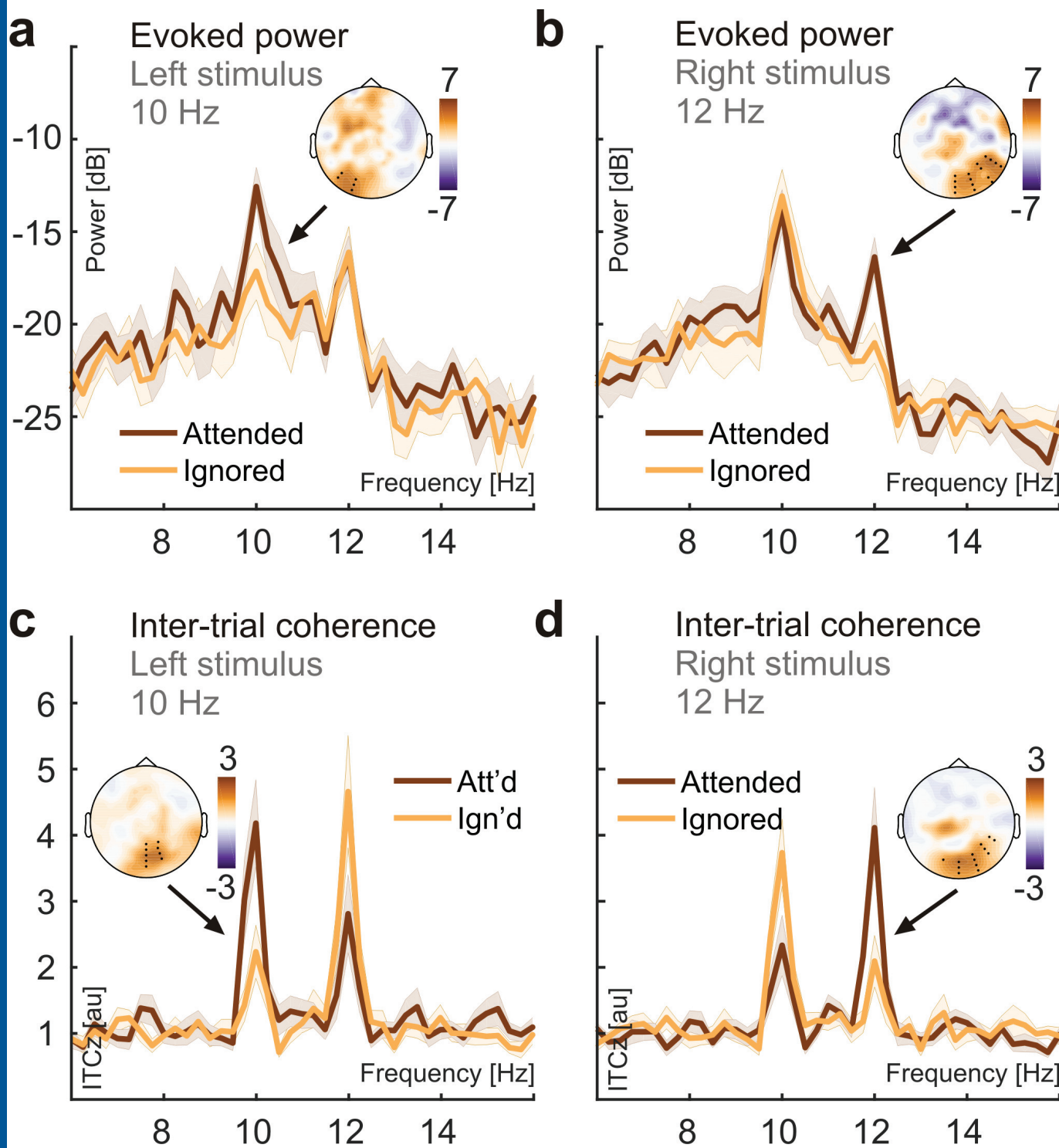
Stimulus cycle



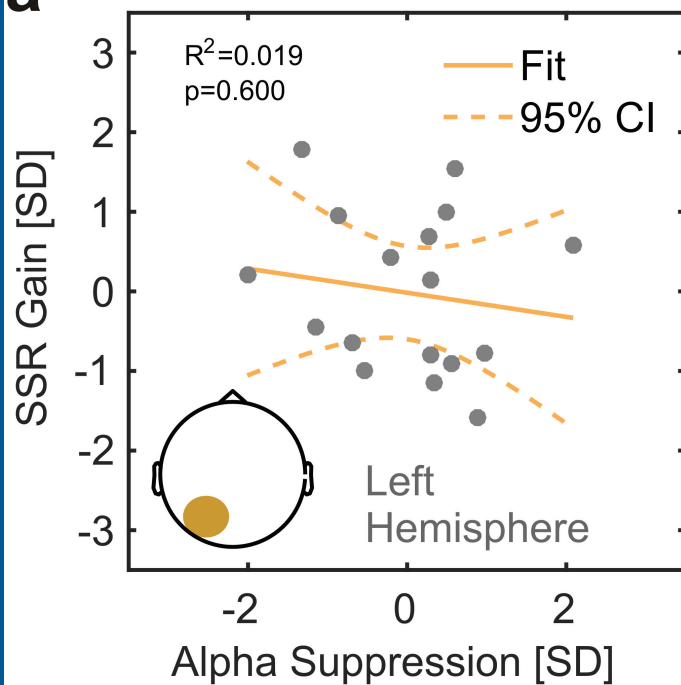




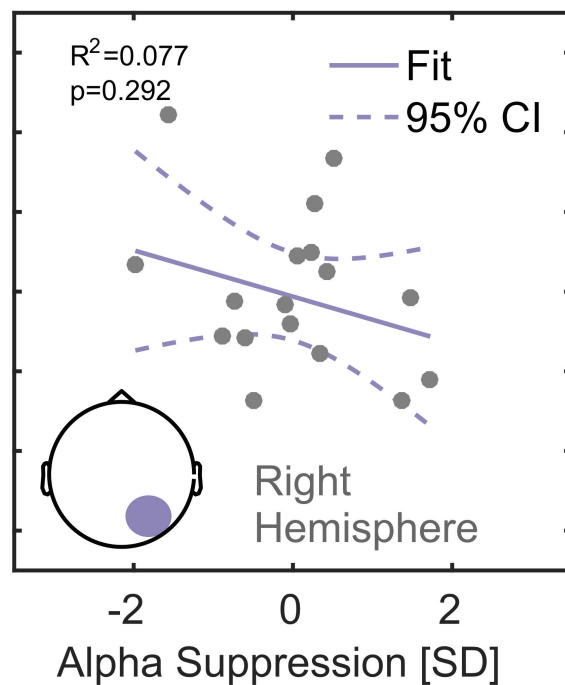




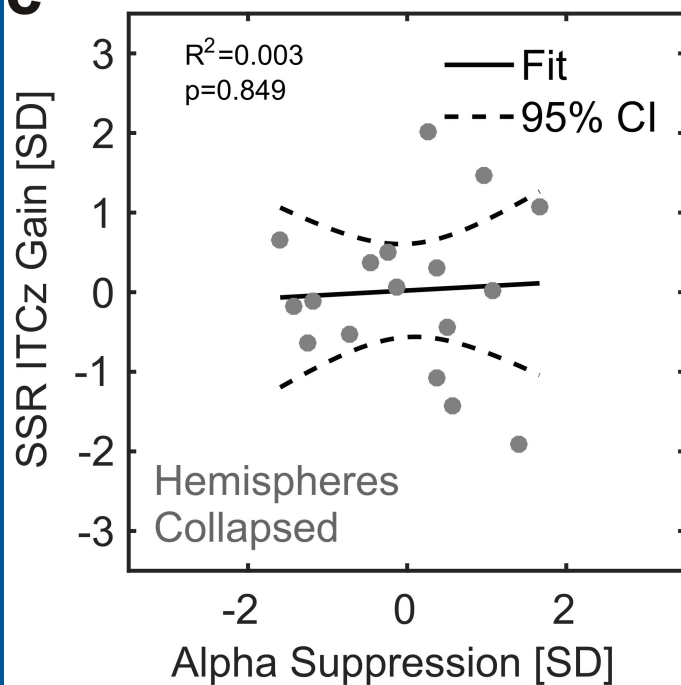
**a**



**b**



**c**



**d**

